SINTECHCOM: Science, Technology and Communication Journal
Vol. 4, No. 2, February 2024, pp. 63-68, DOI: 10.59190/stc.v4i2.261

Negative refractive index anomaly characteristics of SRR hexagonal array metamaterials

Yan Soerbakti[1,*], Moh Danil Hendry Gamal[2], Zamri[1], Defrianto[1], Romi Fadli Syahputra[3]
[1]Department of Physics, Universitas Riau, Pekanbaru 28293, Indonesia
[2]Department of Mathematics, Universitas Riau, Pekanbaru 28293, Indonesia
[3]Department of Physics, Universitas Muhammadiyah Riau, Pekanbaru 28294, Indonesia

ABSTRACT

Metamaterials possess distinct characteristics that make them very suitable for scientific investigation. This phenomenon's hallmark has left scientists perplexed and skeptical. Researchers have conducted numerous studies to explore the composition of one or more metamaterials. This project focused on the development of a linear-sequence metamaterial. Next, we examined the alterations in the optical characteristics of the metamaterial. The utilized frequency range is 0 to 9 GHz. We construct the hexagonal split ring resonance (SRR) metamaterial with a radius of 2.9 mm, consisting of one to four hexagonal SRRs. The findings revealed that the SRR hexagonal metamaterial structure had the highest negative refractive index value, reaching -9.33 in combinations of four hexagonal SRRs.

ARTICLE INFO

Article history:

Received Nov 3, 2023
Revised Jan 9, 2024
Accepted Feb 15, 2024

Keywords:

Double-Negative
Hexagonal
Metamaterial
Refractive Index
Split Ring Resonator

* **Corresponding Author**
E-mail address: yansoerbakti2@gmail.com

1. INTRODUCTION

Many metallic elements arranged at consistent intervals construct metamaterials, which are electromagnetic materials. Reduced dimensions construct metamaterials specifically to interact with electromagnetic waves of the shortest possible wavelengths [1-4]. The reverse Doppler effect refers to metamaterials' ability to modify electromagnetic waves that remain unchanged in their properties when propagating in the opposite direction. The geometry of the metamaterial primarily determines these qualities, not its composition or material [5, 6]. Several names and terminologies refer to metamaterials with negative permittivity and permeability. These include left-handed LH media, media with a negative refractive index, and double-negative (DNG) metamaterials [7-11].

Their distinct atomic arrangements determine the qualities of materials. It is worth noting that nearly all naturally occurring materials exhibit positive permittivity and permeability values across the whole electromagnetic spectrum of metals [12, 13]. Materials with negative characteristics will impede wave propagation because the refractive index becomes imaginary. Materials with negative permittivity and permeability have a refractive index that is both real and negative, which is similar to how waves travel [14-18].

The main idea behind metamaterial sensing is that the transmission and reflection coefficients of the S-parameter (scattering) change frequency [19, 20]. The parameters fluctuate due to changes in the metamaterial resonator's permittivity, permeability, or refractive index. Another technique for sensing relies on phase reflection and transmission coefficients [21-25]. The aim of this study is to investigate abnormalities resulting from the dispersion of refractive index in metamaterials. We employ the Nicolson-Ross-Weir approach to quantify the negative refractive index of metamaterials

using S-parameter transmission and reflection data. We adapted this technique to calculate the permittivity and permeability values of the S-parameters using the CST Studio Suite software and the MATLAB application.

2. RESEARCH METHODS

With the CST software Studio Suites, we will ascertain the specific structural characteristics of the internal metamaterial. This will involve determining the values of T_s (substrate thickness), T_P (patch thickness), c_1 (gap and separation distance between rings), and c_2 (patch width) in order to construct the hexagonal configuration. The next step is to select the constituent components for the metamaterial structure. The components used can include copper for the patch (radiation component) and ground (earthing component), as well as FR-4 as a substrate (dielectric material). We measure the diameters of these components in millimeters (mm). We conducted the hexagonal split-ring resonators (SRR) metamaterial structure design procedure, modifying the radius values R1, R2, R3, and R4 as required. Initially, we will establish the boundary field conditions and excitation sources in order to model metamaterial structures using various combinations of hexagonal SRR, We determine the frequency of observations and initiate the experiment by executing the Start experiment command. We present the simulation results as S-parameter data and then export it to Excel using the *.xlxs file format. Next, we import the data into MATLAB to calculate and display the permittivity, permeability, and refractive index values derived from the data, both in numerical form and through graphical representations.

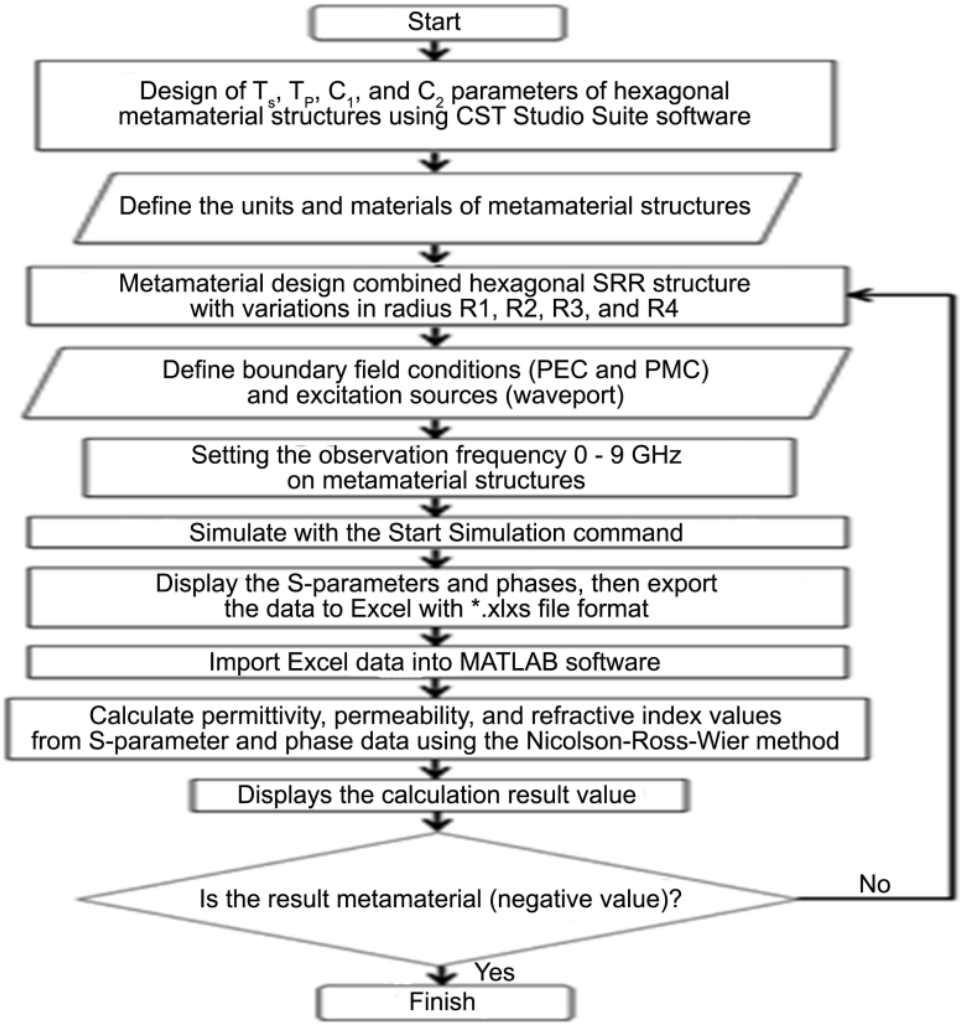

Figure 1. Flowchart for assessing the optical properties of metamaterials.

3. RESULTS AND DISCUSSIONS

The purpose of this investigation was to examine the unique outcomes of two types of metamaterial constructions, one with metal inclusions and one without. We can use the NRW approach to analyze S-parameter data, specifically S11 (reflection) and S21 (transmission), which leads to the identification of DNG (double negative) materials. These materials have negative values without metal, making them a type of metamaterial. We derive the metamaterial's negative properties by analyzing the real component at resonant frequency.

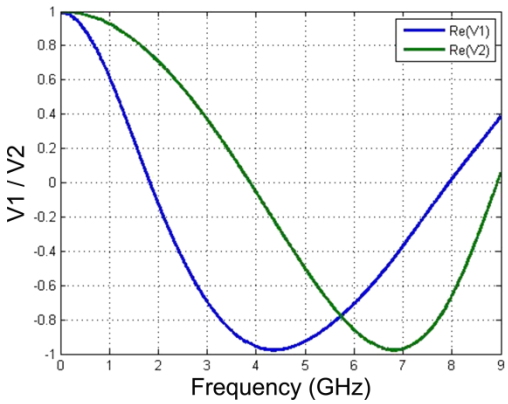

Figure 2. Graph of real parts V1 and V2 of FR4 substrate.

The absorption of electromagnetic wave energy by electron polarization leads to a certain frequency at which material dispersion resonance occurs, resulting in deflection in the same direction. The resonance frequency values Re(V1) and Re(V2) are shown in Figure 2. They are similar to the permittivity and permeability values in Figures 3 (a) and (b). Figure 3 (c) depicts a graph of resonant frequency that closely resembles the resonant frequencies of permittivity and permeability at 4.45 GHz and 6.94 GHz, respectively, based on the refractive index, derived from the square root of permittivity and permeability.

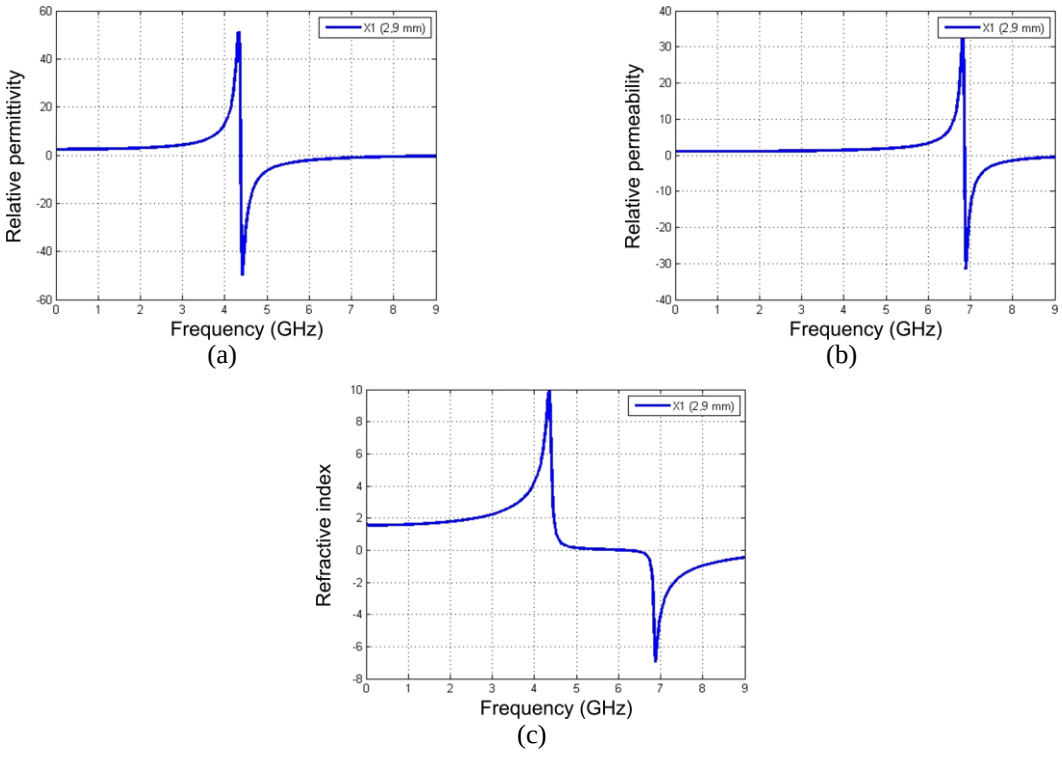

Figure 3. Combination of one hexagonal SRR: (a) permittivity; (b) permeability; and (c) refractive index.

Findings from the study shown in Figure 4 (a), (b), and (c) show that when four hexagonal SRRs are mixed together, the initial resonance frequency causes larger negative values of permittivity, permeability, and refractive index compared to when one to three metamaterials are mixed together. This phenomenon arises due to the introduction of a dielectric medium, which leads to a decrease in the polarization of electrons as a result of the generated electric and magnetic field moments [6]. Consequently, alterations in the material's relative permittivity and permeability have a more significant effect. At a frequency of 1.97 GHz, the refractive index reaches its maximum negative value of -9.33. Augmenting the hexagonal SRR metamaterial structure, particularly at lower frequencies, diminishes the frequency shift. The resonance frequency changes when hexagonal SRR are added. This makes the induction of both the electric (E) and magnetic (B) fields weaker for each structure.

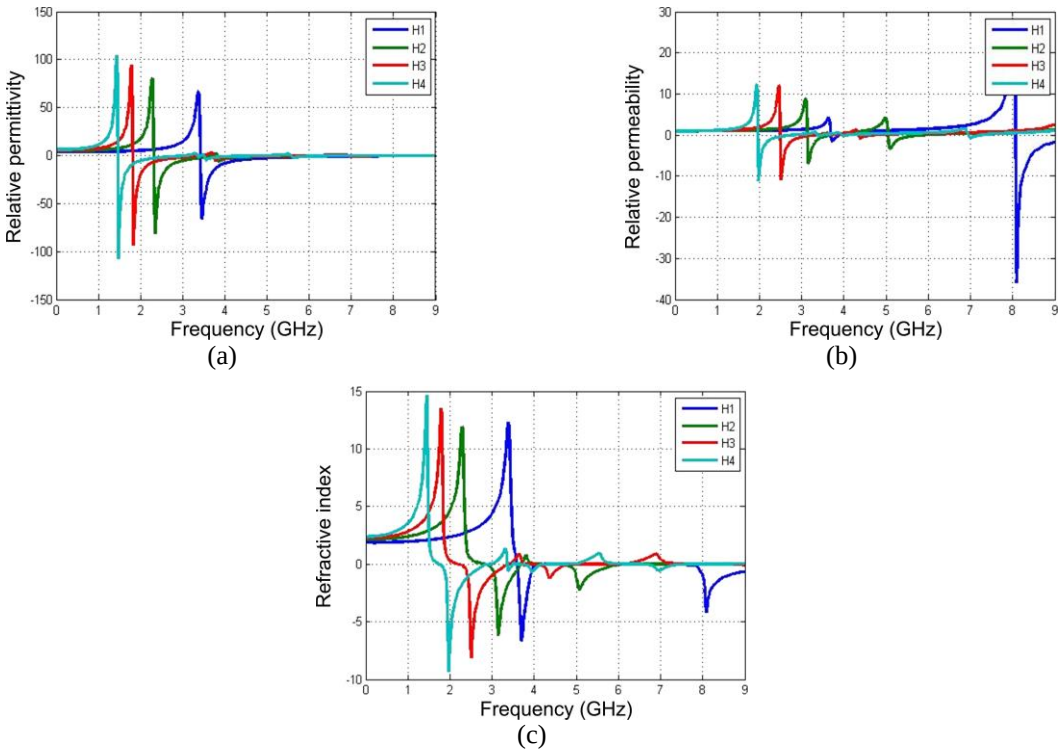

Figure 4. Hexagonal SRR combination: (a) permittivity; (b) permeability; and (c) refractive index.

4. CONCLUSION

Permittivity and permeability only derive their resonant frequencies from the actual components V1 and V2, respectively. Adding metal particles and making the hexagonal SRR metamaterial structure on the substrate bigger cause the resonance to rise and the frequency to move toward lower levels. The negative refractive index grows by 50% as the number of hexagonal SRR metamaterial structures increases from one to four, resulting in a range of values from -6.64 to -9.33.

REFERENCES

[1] Caloz, C. & Itoh, T. (2005). *Electromagnetic metamaterials: transmission line theory and microwave applications*. John Wiley & Sons.

[2] Defrianto, D., Soerbakti, Y., Syahputra, R. F., & Saktioto, S. (2020). Analisis kinerja antena berdasarkan pengaruh variasi kombinasi dan jarijari metamaterial heksagonal struktur split ring resonator. *Seminar Nasional Fisika Universitas Riau V (SNFUR-5)*, **5**(1), 1–4.

[3] Soerbakti, Y., Rini, A. S., Astuti, B., Anita, S., Suyanto, H., & Rati, Y. (2024). Optimization of semiconductor-based SRR metamaterials as sensors. *Journal of Physics: Conference Series*, **2696**(1), 012015.

[4] Saktioto, Soerbakti, Y., Syahputra, R. F., Gamal, M. D. H., Irawan, D., Putra, E. H., Darwis, R. S., & Okfalisa. (2022). Improvement of low-profile microstrip antenna performance by hexagonal-shaped SRR structure with DNG metamaterial characteristic as UWB application. *Alexandria Engineering Journal*, **61**(6), 4241–4252.
[5] Chen, T., Li, S., & Sun, H. (2012). Metamaterials application in sensing. *Sensors*, **12**(3), 2742–2765.
[6] Saktioto, S., Siregar, F. H., Soerbakti, Y., Rini, A. S., Syamsudhuha, S., & Anita, S. (2024). Excellent integration of a multi-SRR-hexagonal DNG metamaterial into an inverted triangle top microstrip antenna for 5G technology applications at 3.5 GHz. *Przeglad Elektrotechniczny*, *2024*(1).
[7] Caloz, C. & Itoh, T. (2004). Transmission line approach of left-handed (LH) materials and microstrip implementation of an artificial LH transmission line. *IEEE Transactions on Antennas and Propagation*, **52**(5), 1159–1166.
[8] Iyer, A. K. & Eleftheriades, G. V. (2002). Negative refractive index metamaterials supporting 2-D waves. *2002 IEEE MTT-S International Microwave Symposium Digest (Cat. No. 02CH37278)*, **2**, 1067–1070.
[9] Soerbakti, Y., Defrianto, D., Rini, A. S., & Asyana, V. (2023). Performance analysis of metamaterial antennas based on variations in combination and radius of hexagonal SRR. *Science, Technology and Communication Journal*, **4**(1), 1–4.
[10] Zamri, Z. & Soerbakti, Y. (2022). Determination of the most effective wifi signal intensity area in an enclosed room. *Science, Technology and Communication Journal*, **2**(2), 69–72.
[11] Musaed, A. A., Al-Bawri, S. S., Islam, M. T., Al-Gburi, A. J. A., & Singh, M. J. (2022). Tunable compact metamaterial-based double-negative/near-zero index resonator for 6G terahertz wireless applications. *Materials*, **15**(16), 5608.
[12] Soerbakti, Y., Saktioto, S., Dewi, R., & Rini, A. S. (2022). A review-Integrasi lapisan tipis ZnO pada aplikasi metamaterial sebagai wujud potensi sensor ultra-sensitif dan multi-deteksi. In *Seminar Nasional Fisika Universitas Riau VII (SNFUR-7)*, **7**(1), 1–9.
[13] Rahayu, Y. & Artiyah, I. (2021). Design and development of microstrip antenna circular patch array for maritime radar applications. *Science, Technology and Communication Journal*, **1**(3), 83–88.
[14] Smith, D. R. & Kroll, N. (2000). Negative refractive index in left-handed materials. *Physical Review Letters*, **85**(14), 2933.
[15] Saktioto, S., Zakky, F., Fardinata, R., Abdullah, H. Y., & Fadhali, M. M. (2023). Equilibrium of argon plasma particles at high pressure. *Science, Technology and Communication Journal*, **4**(1), 21–30.
[16] Roslan, M. S., Zin, A. F. M., Rosley, R., Abdullah, F. B., Amran, N. S., Rosslan, N. J. A., Jameel, M. H., & Haider, S. Z. (2021). Reflective and structural characteristics of natural pearl. *Science, Technology and Communication Journal*, **2**(1), 15–20.
[17] Li, W., Meng, F., Chen, Y., Li, Y. F., & Huang, X. (2019). Topology optimization of photonic and phononic crystals and metamaterials: A review. *Advanced Theory and Simulations*, **2**(7), 1900017.
[18] Wan, B. F., Ye, H. N., Zhang, D., & Zhang, H. (2023). A variable refractive index sensor based on epsilon-near-zero spatial selection structure and its potential in biological detection. *New Journal of Physics*, **25**(2), 023003.
[19] Rezki, Y. P., Syahputra, R. F., & Ginting, D. (2023). Design and testing of circular metamaterial-based salinity sensors. *Science, Technology and Communication Journal*, **3**(3), 79–84.
[20] Fauzan, M., Fardinata, R., & Ramadhan, K. (2021). Microwave media simulation to generate nitrogen plasma at atmospheric pressure. *Science, Technology and Communication Journal*, **2**(1), 21–28.
[21] Soerbakti, Y., Syahputra, R. F., Saktioto, S., & Gamal, M. D. H. (2020). Investigasi kinerja antena berdasarkan dispersi anomali metamaterial struktur heksagonal split ring resonator. *Komunikasi Fisika Indonesia*, **17**(2), 74–79.

[22] Syahputra, R. F., Soerbakti, Y., Syech, R., Taer, E., & Saktioto, S. (2020). Effect of stripline number on resonant frequency of hexagonal split ring resonator metamaterial. *Journal of Aceh Physics Society*, **9**(1), 26–30.
[23] Gamal, M. D. H., Soerbakti, Y., Zamri, Z., Syahputra, R. F., & Saktioto, S. (2020). Investigasi karakteristik anomali indeks bias negatif metamaterial array struktur split ring resonator. *Seminar Nasional Fisika Universitas Riau V (SNFUR-5)*, **5**(1), 1–4.
[24] Wang, Z., Wang, X., & Wang, J. (2021). Research advance on the sensing characteristics of refractive index sensors based on electromagnetic metamaterials. *Advances in Condensed Matter Physics*, **2021**(1), 2301222.
[25] Mostufa, S., Yari, P., Rezaei, B., Xu, K., Sun, J., Shi, Z., & Wu, K. (2023). Metamaterial as perfect absorber for high sensitivity refractive index based biosensing applications at infrared frequencies. *Journal of Physics D: Applied Physics*, **56**(44), 445104.